www.czasopisma.pan.pl PAN POLSKA AKADEMIA NAUK www.journals.pan.pl

A R C H I V E S O F M E T A L L U R G Y A N D M A T E R I A L S

Volume 59 2014 Issue 4

DOI: 10.2478/amm-2014-0234

S. WĘGRZYNKIEWICZ*, D. JĘDRZEJCZYK**, I. SZŁAPA***, M. HAJDUGA**, S. BOCZKAL****

INFLUENCE OF A SUBSTRATE SURFACE ON THE (Zn) – COATING FORMATION

WPŁYW POWIERZCHNI PODŁOŻA NA KSZTAŁTOWANIE SIĘ POWŁOKI (Zn)

The steel substrate was cut by means of different methods, like water jet, laser or oxyacetylene blowpipe. So, some different surfaces (after cutting / without cutting) were subjected to the (Zn) – hot dip galvanizing. The galvanizing process was performed in industrial conditions by applying the constant temperature equal to 457°C, and a dipping time equal to 150 s. The (Zn) – coating morphologies and sub-layer thicknesses were analyzed to explain some expected differences in the coatings formation.

Keywords: hot-dip Zn galvanizing, heat affected zone – HAZ, water jet cutting, oxyacetylene cutting, laser cutting

W prezentowanej pracy podłoże stalowe cięto stosując różne metody: strumień wody, laser, palnik acetylenowo-tlenowy. W wyniku tego otrzymano zróżnicowaną powierzchnię (po cięciu/bez cięcia), którą poddano cynkowaniu ogniowemu. Proces cynkowania wykonywano w warunkach przemysłowych stosując stałe parametry: temperaturę 457°C, czas zanurzenia t=150 s. W trakcie badań analizowano morfologię powłoki cynkowej oraz grubości poszczególnych podwarstw w celu wyjaśnienia różnic w narastaniu powłok.

1. Introduction

It is well known that the hot dip zinc galvanizing process is the most often used in industrial application to protect Fe-C alloys against corrosion influence of aggressive environment. Investigations led from many years solved already a lot of problems but even now some of them can be found in industrial practice of Zn galvanizing that can result in differentiation of coating thickness, increasing defects number and generally decrease the surface quality. Beside others factors also method of forming of the zinc galvanizing elements – cutting process disturbs the kinetic of Zn layer growth on steel. The perfect cutting process is defined as: "a process enabling to divide the atomic bonds in the cutting plain along the determined line, without any influence on physicochemical material's properties" [1]. The cutting methods applied in the industry differ among others in the amount of the consumed energy, the quality of cut edges and the thermal influence on cut material. The basic parameters determining the way of cutting are: the kind and the thickness of cut material, the length and the shape of the line of the cut, the required quality of cut edges surface, production possibilities and costs of the process. Every of applied technologies should ensure: low energy consumption, narrow cutting gap, the possible low influence on structure of cutting material and very good quality of cutting edges [2-4].

Anticorrosion properties of zinc coating that play essential role in protection among others of fittings for overhead power lines are determined by structure of created layer composed normally of few sub-layers. To analyse of the zinc-coating structure created on steel the basis is the Fe-Zn phase equilibrium diagram [5-7]. This diagram for several dozen years underwent many changes. Generally, it was proved, that in Fe-Zn diagram occurs three phases, arising as a result of the peritectic reaction: Γ – Fe_3Zn_{10}, δ – $FeZn_7$, ζ – $FeZn_{13}$ and iron solid solution in zinc – η. Next research referred to different forms of δ – phase existing within different temperature range (δ_1, δ) and with different morphology (δ_C – compacted, δ_P – palisade). Also $\Gamma 2$ phase that is created as a result of reaction between $\Gamma 1$ and δ phases was distinguished [8]. The sequence of phases creation in Fe-Zn diagram and typical Zn coating structure on steel is presented in Fig. 1.

The model of Zn layers growth presented in Fig. 2 is similar to sub-layers structure proposed for Ni/Al/Ni interconnection [10, 11]. Additionally, properly elaborated model can be applied to prediction of the concentration profile of the corresponding bath's components at the sublayers depth [12]. In both cases (Ni/Al/Ni and Fe/Zn) we can observe channels and grooves between created phases, but the main idea consist in explanation that sub-layers start to appear according thermodynamic calculation in determined order. First Al_3Ni_2 phase

* BELOS-PLP S.A., 74 GEN. J. KUSTRONIA STR., 43-300 BIELSKO-BIAŁA, POLAND
** UNIVERSITY OF BIELSKO-BIAŁA, 2 WILLOWA STR., 43-309 BIELSKO-BIAŁA, POLAND
*** BISPOL S.A., 30 TOWAROWA STR., 43-300 BIELSKO- BIAŁA, POLAND
**** INSTITUTE OF NON-FERROUS METALS, 19 PILSUDSKIEGO STR., 32-050 SKAWINA, POLAND

is created than Al_3Ni. So, analogically we can assume that in Fe-Zn system Γ1 phase will be observed as the first one next within few seconds the sub-layer of δ_c and δ_p will be created. The presented mechanism prove that also properties of steel base can influence on the kinetics of Zn coating growth. On the other hand properties of steel surface depends strongly on the cutting method and it's parameters.

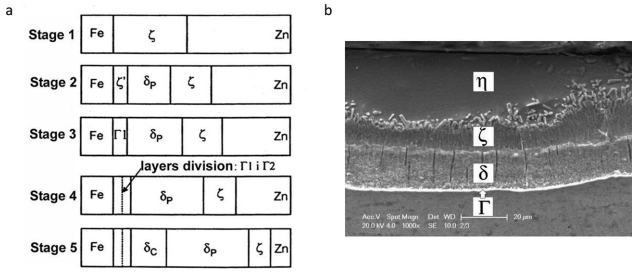

Fig. 1. The sequences of phases creation in Fe-Zn diagram – a [9]; the structure of Zn coating – b [own investigations]

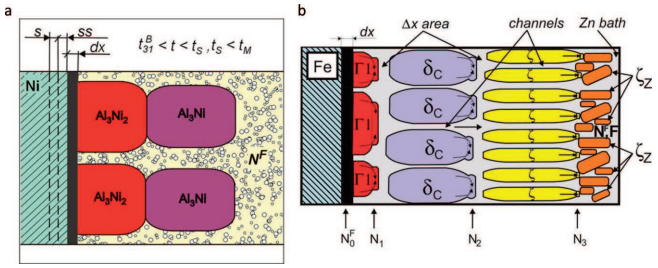

Fig. 2. The model of sub-layers crystallization process: in Ni/Al/Ni interconnection - a [10]; and in Zn coating – b [9]

In available literature there is no the detailed information describing the influence of the state of the surface formed after cutting on the structure and the corrosion resistance of the zinc coating. Only few authors [13, 14] analyzed this problem but only casually. In practice the problem of the Zn coating quality created on elements of power network of overhead lines is important especially considering the operational lifetime [own experiments].

In the industry, in the wide range the following methods are applied: oxyacetylene blowpipe (OAB), laser, water jet or water-abrasive cutting and electrical discharge. Cutting methods differs in the amount of consumed energy, the impact of heat on the material and the quality of the cutting edge [15, 16]. The applied parameters influence among others on the structure and properties of outer layer – that depend on the creation of so-called Heat Affected Zone (HAZ). The HAZ thickness depends above all on process temperature and beam concentration, that next influence on puncture thickness and heating rate of the forming material. For example the beam concentration for OAB is about $10^7 W/m^2$ (plasma – $10^{11} W/m^2$, laser $10^{15} W/m^2$). Corresponding cutting temperature (in material) amounts to: 1050-1380°C – OAB (Fe, 1,5%C steel); 10000°C – plasma (flame); 1200°C – laser; <100°C – water [17]. So, with decreasing the beam concentration the HAZ thickness increases. Moreover, the very important process parameter is cutting rate (with its increasing the HAZ thickness decrease). As the result of OAB cutting the layers with higher hardness surrounds the created cutting gap (even in low carbon steel) and surface hardened in medium carbon steel is observed. In the case of low carbon steel the hardened layer thickness is very low [18, 19].

The thermal impact of beam results in hardening of layers surrounding the cutting kerfs (even in low-carbon steel) and the quenching of the cut surface of steel with higher carbon content [20].

Changes in the structure of the cut material influence on the sublayers thickness proportion and properties of zinc coatings. ISO 1461 and ISO 14713 standards indicate a problem with the achievement of required Zn coating thickness and adhesion in the zones close to thermal cutting surface [21, 22]. This problem is also observed in the production of fittings for overhead power lines. In accordance with the requirements of PN-EN 61 284 fittings for overhead power lines made of steel (except stainless steel) should be protected by hot-dip galvanizing or other method that guarantee similar protection against corrosion [3]. Due to the fact that these products are used in a corrosive environment of varying aggressiveness, it is important to try to reduce described difficulties basing upon the action modifying the forming process. Difficulties in achieving the required thickness of Zn coating and its adhesion to the steel surface forming by flame cutting (OAB), very large differences in the thickness of coatings on the flat/front surfaces and the side surfaces were the reason of this study initiation.

In the presented paper authors described the influence of the way of cutting of steel on the structure and the growth kinetics of the Zn layer created by hot-dip galvanizing on different surfaces of links fittings for overhead power lines – a double eyes links type SLINK made of S355JR steel.

To improve the Zn galvanizing effects the research was conducted in a few directions: elimination of the coating thickness diversification by application of other (apart from OAB) cutting method (water jet, laser – presented inside this work); more thorough cleaning of the steel surface area before galvanizing (electropolishing, grinding), as well as determining the influence of the additional heat treatment on narrowing the differences in the coating structure (next publication).

2. Experimental

2.1. The research object

The study was conducted on links commonly used in fittings (Fig. 3) – made of S355JR steel. Research was focused on a double eyes link type SLINK 626502006. Chemical composition of materials used in experiment is presented in Table 1. Carbon and sulphur were determined using LECO CS-125 analyzer. Other elements were analyzed on the ICP-OES spectrometer.

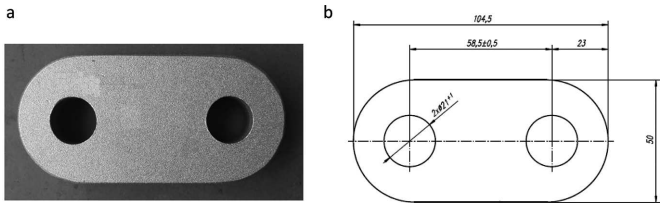

Fig. 3. The view and dimensions of the tested materials – SLINK; a – general view, b – the basic dimensions

TABLE 1

Chemical composition of steel used in the experiment

Source of data	Chemical composition [%]					
	C	Si	Mn	P	S	Cu
PN-EN 100025-2004	$\leqslant 0,24$	$\leqslant 0,55$	$\leqslant 1,60$	$\leqslant 0,035$	$\leqslant 0,035$	$\leqslant 0,55$
Chemical analysis	**0,18**	**0,23**	**1,5**	**0,012**	**0,008**	**0,030**

Preparation of material for galvanizing: three series of links (Fig. 3) were cut from steel sheet with a thickness of 20 mm. The main difference between analyzed series was a method of the material cutting: water jet, laser and OAB. The parameters of applied cutting methods are presented in Table 2.

TABLE 2

Parameters of applied cutting methods

Method of cutting	Cutting tool	Cutting parameters
Water jet	water	Waterjet –Jet EDGE 40°C, υ =82mm/min
Laser cutting	laser	Laser BYSTRONIC – model BYSPEED 3015 power 4kW 1200°C, υ =800mm/min
OAB	oxyacetylene	CNC 500 MESSER 1200°C, υ =400mm/min

After cutting, the prepared materials were subjected to an abrasive blasting – steel shot GL40. In the next stage samples were treated chemically – pickling (hydrochloric acid 12%, 30 g/l Fe), rinsing in cold water and fluxing (TIBFLUX60 – pH 4,9, 0,17 g/l Fe, 292 g/l $ZnCl_2$, 189 g/l NH_4Cl).

Hot-dip Zn galvanizing – Hot-dip Zn galvanizing process was made in industrial conditions in temperature: 457°C and dipping time t=2,5 min in Zn bath enriched in: nickel, bismuth and aluminium. The bath chemical composition was as follows: 99.859% Zn, 0.0481% Ni, 0.0417% Bi, 0.0002% Al, 0.037% Fe, 0.0058% Pb, 0.0014% Sn, 0.0067% Cu, 0.0006% Cd. During the galvanizing of all elements the special attention was paid to maximum repetitiveness of technological process parameters.

3. Results analysis

3.1. Hardness measurement

The hardness measurement was carried out using Vicker's method according to PN – EN ISO 6507 – 2007 [23]. The examination was divided in two stages. In the first stage the hardness (HV10) of side link SLINK surface after cutting was measured. The measurement was made perpendicularly to cutting plane. The average values from a dozen places of the measurement were as follows: water – 155,72 HV10, laser – 416,7 HV10, OAB – 352,4 HV10 – Fig. 4a. In the second stage the hardness measurement (HV0,5) was made starting from the cutting edge toward the sample core. The step of the measurement was established on 200 μm. Results are presented in Fig. 4b.

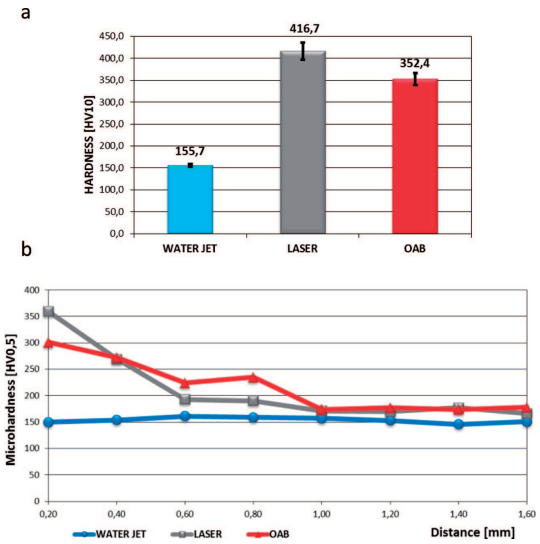

Fig. 4. Results of hardness measurement (HV0,5) on the side surface of links (water jet, laser, OAB): a – HV10 on the side surface perpendicular to cutting plane; b – HV0,5 in direction from cutting edge to the sample core

3.2. Metallographic observations

Metallographic examinations was made for all samples after cutting and hot-dip zinc galvanizing. Metallographic specimens were prepared in classic way. The surface was etched with 4% HNO_3. To optical microscopic observation the microscope AxioImager M1m Carl Zeiss was used with magnification: 50, 100, 200 and 1000x. Chosen results of observation – the structure of base material and Zn coatings are presented in Fig. 5 and Fig. 7. The measurement of Zn coating thickness was made for all samples after galvanizing. Results measured in several places on flat and side surfaces are collected together in Fig. 6.

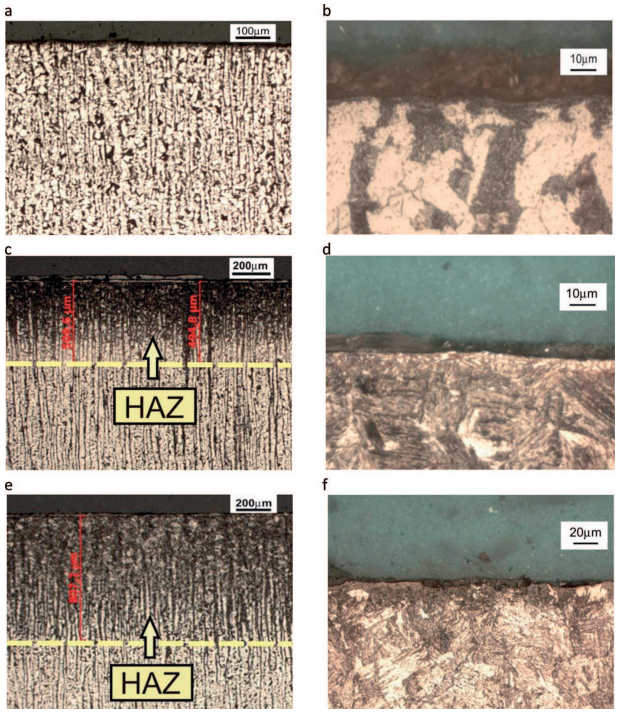

Fig. 5. The cross section of surface layer steel structure (without Zn coating) after different kind of cutting: a, b – water; c, d – laser; e, f – OAB

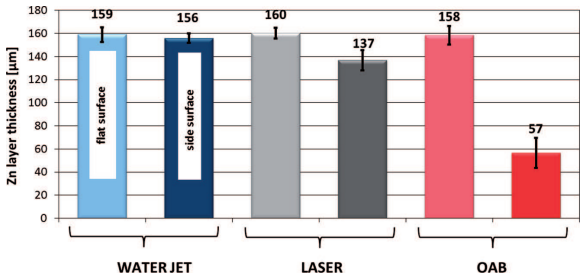

Fig. 6. Diversity of Zn coating thickness with dependence on cutting method

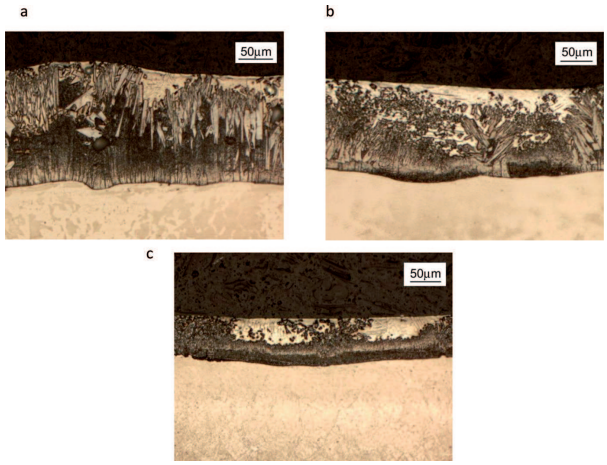

Fig. 7. The cross section of Zn layer created on the steel surface (T=457°C, t = 2,5min) cut using different method: a – water, b – laser, c – OAB

3.3. RTG analysis

Further examination was made with application of scanning microscope "PHILIPS XL30" with X-ray analyzer. The cross section of the steel structure observed after different cutting method before shot blasting and zinc galvanizing is shown in Fig. 8, together with typical EDS graph of the oxides layer generated by thermal impact. Zn distribution that was measured at the coating cross section in points marked in Fig. 9 a, c, e (the measure step was 5-10 μm) is enclosed in Fig. 9 b, d, f.

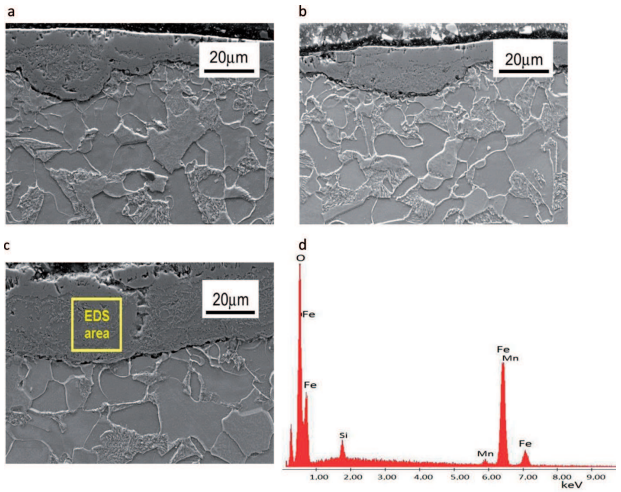

Fig. 8. Comparison of oxide layer created on the steel surface after different cutting: a – water, b – laser, c – OAB; d- EDS graph from area marked in Fig. 8c

4. Results discussion and conclusions

It was stated that the biggest diversification of coating thickness created on the examined elements (layer on the front surface has a thickness three times bigger than on the side surface) appears in the case of the OAB cutting. Laser cut causes decreasing the coating thickness difference to about 25%. In case of water jet cutting there is practically no difference in coating thickness. Observed changes have a close relationship with the microstructure of steel in the surface layer (heat affected zone – HAZ, surface oxidation) which next influences the mechanism and kinetics of the Zn coating growth.

The performed metallographic analysis and hardness measurement confirmed that application of thermal cutting methods results in the hardening of the steel subsurface zone in comparison to values measured in element core, i.e. 155 HV10 (steel S355JR). In the case of surface area cut with water, hardness in compared zones didn't change (Fig. 4). The application of the laser beam caused the surface hardness increase to 400 HV10, cutting by gas flame increased the hardness to 350 HV10 (Fig. 4).

The structure of the material in the initial state was a little bit anisotropic, mainly ferritic with small amount of pearlite – Fig. 5a, b. In the observed HAZ zone the needle shape structure appeared – lower bainite, martensite (in the subsurface zone of sample cut with laser: fine-needle, cut with OAB: coarse – needle – Fig. 5c-f) created as a result of undesirable quenching treatment caused by cutting.

The decarburized layer in the sample after laser cutting is narrow and its thickness amounts to 3 μm. In the subsurface zone of sample where the OAB cutting was applied there is no evident decarburization zone but only oxides layer can be distinguished being the product of reaction proceeded during flame cutting.

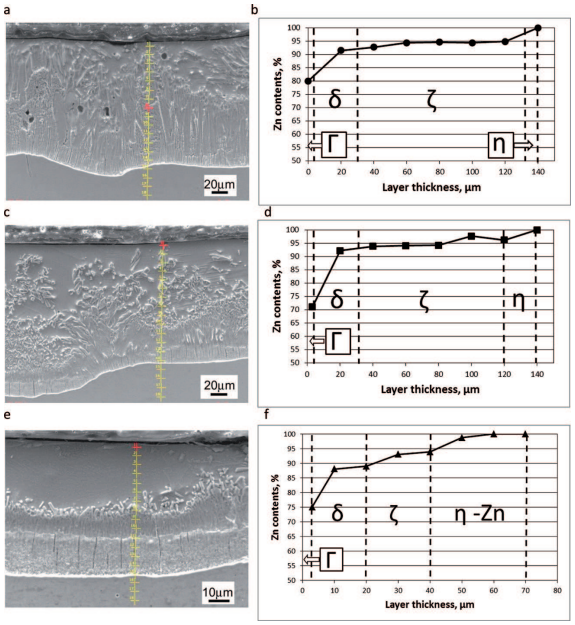

Fig. 9. The microstructure and Zn distribution at the cross section of the coating created after different cutting method: a, b – water; c, d – laser; e, f – OAB

The size of the HAZ in the subsurface layer of samples cut both with laser and OAB was determined on the basis of

microscopic observations – typical changes in the steel structure from ferritic-pearlitic to bainite, martensite (see Fig. 5). The HAZ area boundary in both cases is distinct and is running parallel to cut edge.

In the case of the flame cutting the HAZ thickness amounts to 0,8 – 1,8 mm, whereas in the sample cut with the laser, HAZ is narrower and its thickness amounts to 1 mm. The compared effects results mainly from differences in the cutting rate (laser – υ =800 mm/min, OAB – υ =400 mm/min) because the maximal values of temperatures gained in cutting area in both cases can differs slightly (ab. 1200°C).

The thickness of the coating on flat/front surfaces of all tested elements – links was stable and amounted to ab. 160 μm (Fig. 6). The measurement of the coating thickness on the side surface of the sample cut by water revealed values similar to the average. The greater deviation from the value get on the flat surface was stated for side surfaces in samples cut by laser and OAB. The zinc coating created on the side surface formed by gas flame is characterized by a thickness even about 100 μm smaller (Fig. 6) in relation to the flat surface.

Microscopic observation also confirms the diversification of Zn coating thickness and its structure – Fig. 7. The most developed alloyed structure is visible in the coating created on steel surface cut by water jet. Proceeding from water jet cutting through laser forming to OAB cutting method it is clear that the created alloyed layer stay more and more narrow.

The crude steel surface formed by cutting is in every case covered by oxides – Fig. 8. It is very interesting that despite the relatively low temperature (40-100°C) also on the steel surface cut by water jet the thin oxide layer appears that can influence kinetic of Zn layer growth. It suggest the assumption that remains of oxide layer can't be the only one reason of Zn coating structure changes. The typical EDS graph (similar and typical for oxides layers on every cut surfaces) registered in created oxide layers on OAB cut surface is presented in Fig. 8d.

The Zn coating put on the surface after cutting by water reveals typical structure for this grade of steel – composed of phases: Γ, δ, ζ and η (Zn) – Fig. 9. Layers created by iron diffusion ($\delta + \zeta$) occupies the greater part of the coating thickness (130μm – 80% of total thickness). The coating growth was not disturbed/hindered by the heat affection results of cutting (there is no HAZ) and the application of shot-blasting before galvanizing additionally supported proper process course. In the case of the coating created on the surface cut by laser the alloyed layer ($\delta + \zeta$) has similar thickness (120 μm – 75% of total thickness). Only in the case of Zn coating created on the surface after OAB cutting the observed structure is quite different – the alloyed area is much more thinner (40 μm – 50% of total thickness) – the rest is occupied by pure zinc. It looks like HAZ zone – its higher hardness, different steel surface structure (bainite, martensite) or thicker oxide layer being the product of reactions in higher temperature and longer time during cutting (not precisely removed from the treated surface) disturb/hinder diffusion process on the Zn coating/steel surface.

On the basis of investigation results and its discussion the following conclusions can be formulated:

1. The tested cutting methods (water jet, laser, OAB) influence essentially on the growth kinetics of Zn layer on the face of cut of steel. After the water jet and laser cutting the greatest part of coating cross section is occupied by the ζ phase (correspondingly 105 and 90 μm), while after the OAB cut the thickness of ζ phase amounts only to 20 μm. The thickness of δ phase in all cases is similar (20 μm – OAB; 30 μm – water and the laser). The smallest thickness of η phase was measured for the coating after the water cutting (5-10 μm), in case of OAB cutting this phase thickness reaches 30μm, in the coating on steel cut with the laser thickness η amounts to 20 μm.
2. The reduced iron diffusion rate to Zn coating on the cut side surface is probably a reason for diversifying both thickness of the entire coating and its individual sublayers due to reduction of the solubility of the steel basis resulting from the creation of HAZ zone. Also the insufficient cleaning of the steel surface after OAB or laser cutting – remaining oxide layers can create the barrier hindering the diffusion process.
3. To clarify the mechanism suppressing the diffusion of iron to the Zn coating in further research the following experiments are planned: to conduct the heat processing which will remove the HAZ zone; to apply more intensive treatments of cleaning the surface after the cut with the laser and OAB through the grinding and electro-polishing and determination of the influence of introduced process changes on the growth kinetics of the Zn coating.

To confirm the explanations proposed above in the next step of investigation also the corrosion resistance tests are planned inside the salt chamber with application of Zn coatings created on different steel cut faces.

REFERENCES

[1] A. Klimpel, Spawanie, zgrzewanie i cięcie metali, WNT, 2006.
[2] PN-EN ISO 14713-2:2010 Powłoki cynkowe – Wytyczne i zalecenia dotyczące ochrony przed korozją konstrukcji ze stopów żelaza – Część 2: Cynkowanie zanurzeniowe.
[3] S. Węgrzynkiewicz, M. Hajduga, D. Sołek, J. Masalski, Wpływ przygotowania powierzchni stali 30MnB4 na strukturę i ciągłość powłoki Zn uzyskanej w procesie cynkowania ogniowego, Ochrona przed korozją **4-5**, 181-185 (2011).
[4] J. Wesołowski, Powłoka cynkowa na stali – powstawanie, budowa i właściwości, portal-cynkowniczy.pl 2008.
[5] O. Kubaschewski, Iron-Binary Phase Diagrams. Berlin, Springer-Verlag 1982.
[6] P.B. Burton, P. Perrot, Phase Diagram of Binary Iron Alloys. American Society for Metals, Metal Park. OH, 459-466 (1993).
[7] T.B. Massalski, Binary Alloy Phase Diagrams. ASM International, 1990.
[8] D. Kopyciński, E. Guzik, Powłoka cynkowa na powierzchni odlewu z żeliwa sferoidalnego. Inżynieria Materiałowa, 6, 2008.
[9] D. Kopyciński, Monograph, AGH Kraków, 2006.
[10] W. Wołczyński, E. Guzik, J. Janczak-Rusch, D. Kopyciński, J. Golczewski, H.M. Lee, J. Kloch, Morphological Characteristics of multi-layer/substrate systems, Materials Characterization, **56**, 274-280 (2006).

[11] W. Wołczyński, E. Guzik, K. Kurzydłowski, J. Kloch, J. Janczak-Rusch, Macro/Micro Gradient of Solute Concentration during Solidification of the Ni-Al-Ni Interconnections, Archives of Metallurgy and Materials **50**, 231-240 (2005).

[12] W. Wołczyński, J. Janczak-Rusch, J. Kloch, T. Rutti, T. Okane, A Model for Solidification of Intermetallic Phases from Ni-Al System and its Application to Diffusion Soldering, Archives of Metallurgy and Materials **50**, 1055-1068 (2005).

[13] V. Kulik, Povlaky žárového zinku na pálených Plochach, 17 konference zaroveho zinkovani, Ostrava, Czech Republic, 26-38 (2011).

[14] S. Sepper, P. Peetsalu, V. Mikli, M. Saarna, The effect of substrate microstructure on morphology of zinc coatings, 8th International DAAM Baltic Conference, INDUSTRIAL ENGINEERING, Talin, Estonia, 2012.

[15] A. Mazurkiewicz, Wybrane właściwości warstwy wierzchniej po przecinaniu różnymi metodami, TRANSCOMP, XIV International Conference Computer Systems Aided Science, Industry and Transport, 2164-2172 (2010).

[16] S. Zaborski, T. Stechnij, Laserowe i plazmowe cięcie blach ze stali niestopowych i kwasoodpornych Inżynieria Maszyn **4**, 16, 109-116 (2011).

[17] J. Sobieszczański, Spajanie, OWPW, Warszawa 2004.

[18] P. Liberski, H. Kania, P. Podolski, J. Mendala, A. Talarek, Rola warstwy zewnętrznej powłoki cynkowej w ochronie stopów żelaza przed korozją Ochrona przed korozją **4**, , 132 (2006).

[19] D. Jędrzejczyk, M. Hajduga, S. Węgrzynkiewicz, W. Skotnicki, Influence of the surface state on hot dip Zn galvanizing of iron alloys, Metal 2012, Brno, Czech Republic, 2012.

[20] S. Trela, Badania wpływu cięcia laserowego na twardość stali nisko- i średniowęglowych, Mechanik **12**, 77, 877-878 (2004).

[21] PN-EN ISO - 1461:2011 Powłoki cynkowe nanoszone na wyroby stalowe i żeliwne metodą zanurzeniową – Wymagania i metody badań.

[22] PN-EN ISO 14713-2:2010 Powłoki cynkowe – Wytyczne i zalecenia dotyczące ochrony przed korozją konstrukcji ze stopów żelaza – Część 2: Cynkowanie zanurzeniowe.

[23] PN-EN ISO 6507-1:2007 Metale – Pomiar twardości sposobem Vickersa – Część 1: Metoda badań.

Received: 20 December 2013.